THESIS FOR THE DEGREE OF DOCTOR OF PHILOSOPHY

On pilot-based estimation of phase noise

Björn Gävert

CHALMERS
UNIVERSITY OF TECHNOLOGY

Department of Electrical Engineering
Chalmers University of Technology
Gothenburg, Sweden, 2025

On pilot-based estimation of phase noise

Björn Gävert
ISBN 978-91-8103-189-8

Acknowledgements, dedications, and similar personal statements in this thesis, reflect the author's own views.

Doktorsavhandlingar vid Chalmers tekniska högskola
Ny serie nr 5647
ISSN 0346-718X

Department of Electrical Engineering
Chalmers University of Technology
SE-412 96 Gothenburg, Sweden
Phone: +46 (0)31 772 1000

Cover:
A pair of stylish pilot sunglasses to illustrate the importance and coolness of pilot-based phase noise estimation.

Printed by Chalmers Digital Printing
Gothenburg, Sweden, April 2025

On pilot-based estimation of phase noise

Björn Gävert
Department of Electrical Engineering
Chalmers University of Technology

Abstract

There is an ever-increasing demand for higher data rates in wireless communication systems for supporting, for example, the growing consumption of video streaming in today's networks, and extremely data-intensive applications such as immersive communications in future networks. However, wireless communication equipment providing higher rates comes with more stringent hardware requirements. A large contributor to distortion is the phase noise related to up- and down-converting of signals to and from radio frequency. The main focus of this thesis is related to handling the carrier phase noise, balancing complexity and performance. For this, different alternatives for close-to-optimal low complexity pilot-based phase noise estimation methods are studied.

First, a seemingly simple approach is examined in Paper A, where a pilot tone in the form of a sinusoid is added to an unknown communication signal. The power of the transmitted signal is shared between the pilot tone and the communication signal. Several pilot-based phase noise estimation algorithms are studied, and an optimal signal-to-pilot power ratio is presented.

Second, pilot-based phase noise estimation of an OFDM signal affected by phase noise is studied in Paper B. The known pilots are allocated in the frequency domain and occupy a number of subcarriers within the OFDM symbols. A novel, low-complexity pilot-based phase estimator is proposed, which is close to optimal over a wide dynamic range of phase noise levels and signal-to-noise ratios.

Finally, Paper C examines the maximum rate of a line-of-sight MIMO system affected by phase noise, where known pilots are interleaved in the time domain together with the payload. To maximize the rate, a novel pilot-based estimator is proposed that jointly estimates both payload and phase noise.

Keywords: Wireless communication, carrier synchronization, phase noise, frequency domain pilots, time domain pilots, OFDM, MIMO systems

To my wife Anette, my mother Inger, and to my daughters Molly, Tyra and My.

List of Publications

This thesis is based on the following publications:

[A] **Björn Gävert**, Thomas Eriksson, "Estimation of Phase Noise Based on In-Band and Out-of-Band Frequency Domain Pilots". Published in IEEE Transactions on Communications, Volume: 70, Issue: 7, July 2022.

[B] **Björn Gävert**, Mikael Coldrey, Thomas Eriksson, "Phase noise estimation in OFDM systems". Published in IEEE Transactions on Communications, 2024 Early Acces.

[C] **Björn Gävert**, Mikael Coldrey, Thomas Eriksson, "Analysis and Mitigation of Phase Noise in a Line-Of-Sight MIMO System". Submitted to IEEE Transactions on Communications.

Contents

Acknowledgments

Nearly 25 years after completing my master's degree, I returned to academia. After many years working as an engineer, I had grown accustomed to taking shortcuts and thinking, *If it works most of the time, it's OK.* In *Star Wars* terms, this mindset was like the dark side of the Force. It was often powerful but clouded my academic Jedi judgment. Returning to academia has been a long and challenging journey, much like becoming a *Jedi Knight* again and rebuilding my connection to the academic Force.

First of all, I want to express my deepest gratitude to my supervisor, Professor Thomas Eriksson. You're truly brilliant! I can safely say you patiently managed to teach an old dog new tricks. You helped pull me out of the dark engineering side and set me on my path back to academia. Even though my engineering instincts are still there, you have shown me how to control and harness them in a much more powerful way.

I am really grateful to Adjunct Professor Mikael Coldrey for being my co-supervisor. You have an incredible mind and a rare talent for making even the most complex concepts easy to understand. Our discussions have covered everything from academic topics to family and children, and I have truly appreciated them. I could not have done this research without your guidance.

I am really thankful to Professor Erik Agrell for all your support, guidance, and patience with my disorganized mind. You have taught me so much, from research and structuring my academic work to understanding environmental issues and reminding me to focus more on my family.

I am really grateful to Professor Erik Ström. You are one of the most brilliant people I know, not just in your academic work but also in how you connect with others. You truly made all the difference when I was close to hitting rock bottom. Also, thank you for teaching one of the best Ph.D. courses, Advanced Digital Communication.

I would like to express my gratitude to Professor Tomas McKelvey for your excellent Ph.D. courses in linear algebra and estimation theory, as well as for the many valuable discussions we had about my research. I am also grateful to Professor Giuseppe Durisi for providing an outstanding Ph.D. course in information theory. Additionally, I sincerely appreciate Professor Balázs Kulcsár for patiently introducing me to control theory in the Ph.D. course Linear Systems.

I want to express my gratitude to all my colleagues in the department,

including all professors and postdocs. My deepest appreciation goes especially to my office mates, Charitha, Jafar, and Azadeh. Thank you for all the joyful discussions and laughter.

I am grateful to Ericsson as a company and to all my wonderful colleagues there. Few companies give seasoned professionals the opportunity to learn new, advanced skills at this level. You have supported me from day one, and I am proud to be part of Ericsson.

I am truly grateful to have such supportive and patient friends. Your inspiration and encouragement have been invaluable throughout this journey, even though I have become less social over time. Special thanks to the members of *pokergänget* for your unwavering support.

Last but not least, I want to express my deepest gratitude to my brilliant wife. Fortunately, you have been patient with my struggles and have supported me through the nearly psychotic ups and downs of writing papers and participating in PhD courses. The high points have been soaring, while the low points have nearly hit rock bottom. My lovely children have helped me stay grounded and focus on other important aspects of life. My mother has been my guiding light, listening patiently every day to my academic challenges. My sisters have also been incredibly supportive, always lending an ear to my struggles and encouraging me on my journey.

Acronyms

ADC	Analog to digital converter
AR(1)	First order autoregressive process
AWGN	Additive white Gaussian noise
BB	Baseband
BER	Bit error rate
BS	Base station
CPE	Common phase error

CP	Cyclic prefix
CRLB	Cramer-Rao lower bound
CSI	Channel state information
CW	Continuous wave
DAC	Digital to analog converter
DC	Direct current
DFT	Discrete Fourier transform
EE	Energy efficiency
EKF	Extended Kalman filter
EM	Expectation maximization
FIR	Finite impulse response
ICI	Inter carrier interference
IID	Independent and identically distributed
ISI	Inter symbol interference
LDPC	Low density parity check (code)
LOS	Line of sight
LS	Least squares
MIMO	Multiple input multiple output
ML	Maximum likelihood
MMSE	Minimum mean square error
MU	Multi user
OFDM	Orthogonal frequency division multiplexing
PB	Passband

PCA	Principal component analysis
PDF	Probability density function
PDP	Power delay profile
PLL	Phase locked loop
PSD	Power spectral density
RF	Radio frequency
Rx	Receive or receiver
SC	Single carrier
SER	Symbol error rate
SISO	Single input single output
SNDR	Signal to noise and distortion ratio
SNR	Signal to noise ratio
SPR	Signal to pilot power ratio
STBC	Space time block code
SVD	Singular value decomposition
Tbps	Terabits per second
Tx	Transmit or transmitter
UE	User equipment
ULA	Uniform linear array
VCO	Voltage controlled oscillator
WSS	Wide sense stationary

Part I

Overview

CHAPTER 1

Introduction

1.1 Background and motivation

Wireless communication has become an integral part of modern society, facilitating both human and machine interactions. Historically, wireless communication primarily relied on analog equipment, whereas modern systems are dominated by digital processing. The fifth generation of mobile network equipment continue to being deployed, while the foundation for the sixth generation is being established [1]–[3]. As noted in the Ericsson mobility report [4, Figure 5], mobile traffic will continue to grow, increasing the pressure and requirements on mobile networks. Furthermore, with the widespread deployment of radio communication equipment, power consumption is becoming an increasing concern. Thus, alongside the goal of increasing data rates, there is a strong interest in improving energy efficiency (EE). Various aspects of EE are analyzed and discussed in [5].

Higher data rates can be achieved by enhancing spectral efficiency within already deployed frequency bands, thereby driving radio equipment requirements. In fact, there is even great interest in increased rates in already installed equipment without replacing the hardware. Furthermore, there is an

increasing interest in wireless communication equipment operating on higher carrier frequencies where more bandwidth is available, while still maintaining spectral efficiency. However, hardware-related distortion in a wireless communication system is a significant problem when improving spectral efficiency, [6]. One major source of distortion is random time-dependent phase uncertainty, commonly referred to as phase noise, arising from the up- and down-conversion of signals to and from radio frequencies (RF). The severity of phase noise distortion typically increases with carrier frequency [7, Eq. 12 and 13]. Hence, the requirements on phase noise are becoming more stringent with the increasing demands on spectral efficiency and rates, and processing related to estimating and suppressing phase noise is an important subject.

Phase noise degradation can be mitigated through the use of better performing oscillators or advanced phase estimation algorithms. However, as noted in [7], enhancing oscillator performance generally leads to higher power consumption and increased costs (e.g., greater hardware complexity). Similarly, more advanced phase noise estimation algorithms tend to increase signal processing complexity, power consumption, and system latency. The industrialized system often uses a compromise that balances reasonable performance degradation, complexity, and power consumption.

Phase estimation in wireless (and optical) systems has been extensively studied in the scientific literature. An overview of phase noise modeling and phase noise estimation in wireless communication systems is presented in [8, Sections 3 and 4]. Depending on the type of system, there exist many different methods for handling the distortion related to phase noise, where phase noise estimation is performed either in the time domain or in the frequency domain. The modulated RF signal, [9, Sections 10 and 11], carries user data, often denoted payload, which is unknown from the perspective of radio communication equipment. However, the structure of the transmitted signal, for example, the signal bandwidth and the type of modulation [9, Section 11], is normally known by radio communication equipment. Together with the unknown payload, pilot signaling, [10], is often introduced, where pilots act as well-defined anchor points, e.g., known 4 QAM symbols. The known pilots and possibly also soft or hard decisions on the payload are often used when estimating the phase noise of the received and demodulated signal, [9, Section 12].

The received noisy and distorted payload contributes with great uncertain-

ties (e.g., decision errors), which must be treated with great consideration. Due to these uncertainties, phase noise estimation based on the payload typically employs an iterative approach, progressively refining the payload estimate by compensating for phase noise. By iteratively improving the phase noise estimate, the effect of phase noise degradation can be reduced. Due to the iterative nature, the resulting phase estimation algorithms become complex and introduce delay. Furthermore, at low signal-to-noise ratios (SNR), errors related to additive noise can be dominating, which can have a devastating effect on the resulting phase estimates (the noise causes a significant number of symbol errors). Therefore, methods for estimating phase noise based on payload also often include error-correcting codes, resulting in even greater complexity and more significant delay. See also Section 4.1.

In order to significantly reduce complexity of the phase noise estimation, the uncertainties of the payload can be omitted by considering pilot-based phase noise estimation. Since pilot signaling inherently is an overhead to the communication signal, the performance of pilot-based estimator is important, i.e., to achieve the best possible performance for a relatively small overhead. Thus, achieving near-optimal pilot-based phase noise estimation with low (or reasonable) complexity is highly desirable. It should also be noted that a well-performing pilot-based estimation can be of interest even for estimators based on payload. In this thesis, several pilot-based phase estimators are presented and analyzed for different types of wireless communication systems, see Sections 4.3, 4.4 and 4.5.

1.2 Thesis outline

Part I:
The research topics of this thesis are introduced and motivated in Chapter 1. A wireless communication system affected by phase noise is described in Chapter 2. Wireless multi-antenna communication is described in Chapter 3. Several aspects related to the research are presented and summarized in Chapter 4. Chapter 5 contains a summary of the included papers with corresponding author contributions, and concluding remarks and future work are presented in Chapter 6.

Part II:
Contains all included papers, Paper A, Paper B and Paper C.

1.3 Notation

Scalar variables are denoted with lowercase letters, e.g., the scalar complex rotation $e^{i\phi}$. Vectors are denoted with bold lowercase letters, e.g., the signal vector $\boldsymbol{x}$. If necessary, the length of a vector is explicitly stated in the text. Matrices are denoted with bold uppercase letters, e.g., the discrete Fourier transform matrix $\boldsymbol{F}$. If necessary, the size of a matrix is explicitly stated in the text.

Vectors and matrices are either random or deterministic, and no special notation is used for either type. Instead, the text related to each equation clearly defines whether a variable is deterministic or random.

The time index of time varying scalars, vectors and matrices is denoted by subscript, e.g., the symbol vector at time index n $\boldsymbol{s}_n$. Time index is also, when necessary, denoted with parenthesis, e.g., the scalar signal at time index n $s_{\mathrm{RF}}(n)$.

CHAPTER 2

A short description of a wireless communication system

A wireless communication system is designed to transmit data bits between a transmitter and a receiver over a wireless channel. Data typically consists of independent bits with equal probability, originating from sources such as voice, streamed video, or any other form of digital communication service[1].

The model in Figure 2.1 represents a complex baseband system. In a complex baseband representation, an RF passband signal is modeled using complex numbers, omitting the carrier frequency. Complex baseband is closely related to its real passband counterpart[2] [11, Chapter 7]. The wireless communication model is time-discrete and includes a transmitter, a channel, and a receiver. This simplified modeling approach, [9, Section 10.2], includes parts relevant to the research presented in this thesis. In this case, the model contains the phase noise of the transmitter and receiver, modeling the phase noise distortion related to the transmitter up-conversion to RF and receiver down-conversion from RF. The distortion related to hardware imperfections in

[1] Notation in this short introduction follows [9].

[2] Using a time-discrete representation, the physical, existing passband signal, $s_{\mathrm{PB}}(n)$, is related to the complex-valued baseband signal, $s_{\mathrm{BB}}(n)$, according to $s_{\mathrm{PB}}(n) = \Re\{s_{\mathrm{BB}}(n)e^{i2\pi f_c n}\}$.

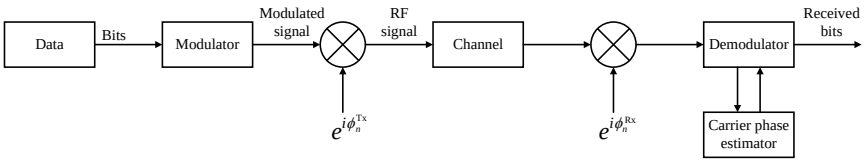

Figure 2.1: A SISO wireless communication model with phase noise.

power amplifiers, analog filters, and other analog components is omitted. Simplified time-discrete baseband modeling of systems for analyzing phase noise distortion, while leaving out distortion from other components, is common in the literature; see, for example, [12], [13], [14], and [15].

A single-input single-output (SISO) wireless communication system, illustrated in Figure 2.1, models a single stream of information transmitted over a wireless channel with one transmitter antenna and one receiver antenna. The SISO system consists of a modulator, transmitter phase noise, a noisy channel, receiver phase noise, and a demodulator. The modulator is described in Section 2.1, and the demodulator in Section 2.4. The wireless channel is detailed in Section 2.2, and phase noise modeling is covered in Section 2.3.

2.1 Modulator

As described in [9, Section 19], the modulator transforms digital information into symbols, which are mapped to analog waveforms. In the simplified time-discrete modeling, Figure 2.1, the output of the modulator corresponds to complex numbers representing the modulated signal.

This thesis includes two modulation schemes: single carrier (SC) modulation [9, Section 11.3.5] and orthogonal frequency-division multiplexing (OFDM) [9, Section 19].

2.2 Channel

The channel models used in this research exhibit slow variations (block fading) and are represented as finite impulse response (FIR) filters [9, Section 7.3.1],

as described by

$$s_{\mathrm{Ch}}(n) = (h * s_{\mathrm{RF}})(n), \tag{2.1}$$

where the channel impulse response, h, is convolved with the transmitted signal $s_{\mathrm{RF}}(n)$. From a channel perspective, two types of wireless communication systems are considered in this thesis. One type of system corresponds to fixed radio with high-gain (parabolic) antennas mounted on tall masts, which is commonly used in wireless backhaul systems. The other system corresponds to mobile access, i.e., user equipment (UE) communicating with a base station (BS). The fixed radio channel is, due to the high-gain antennas, dominated by a line-of-sight (LOS) component which varies slowly. Hence, the LOS system has a channel with low delay spread, suffering mostly from flat fading, and is, therefore, modeled as a single-tap complex gain. Conversely, the mobile access system reflects diverse urban radio conditions and is modeled as an FIR filter with normal distributed taps, which remain constant over a given time period, i.e., a block Rayleigh fading channel. The power delay profile (PDP) of the Rayleigh fading channel is assumed to have exponential decay, i.e., the filter taps of the corresponding channel have a square average amplitude that decays exponentially, as shown in [9, Section 7.3.2 Eq. (7.4)].

The channel also contributes with additive white Gaussian noise (AWGN), which in the case of baseband modeling corresponds to independent and identically distributed (IID) complex rotation invariant Gaussian variables which are added to the received RF signal after channel filtering, according to

$$s_{\mathrm{Noise}}(n) = s_{\mathrm{Ch}}(n) + w(n). \tag{2.2}$$

2.3 Phase noise

As mentioned above, with complex baseband modeling, the RF is "left out" and the RF signal is represented as complex numbers centered around zero frequency. However, oscillators responsible for generating the carrier sinusoid used in signal up- and down-conversion introduce time-dependent phase uncertainties [7], stemming from analog hardware imperfections. The time-dependent phase uncertainty of the oscillators, usually denoted as phase noise, is often modeled as stochastic processes. In a complex baseband representation, phase noise induces a rotational distortion on transmitted and received

RF signals, modeled as an exponential factor $e^{i\theta_n}$, given by

$$s_{\mathrm{PN}}(n) = s(n)e^{i\theta_n}, \tag{2.3}$$

where the phase noise is represented by θ_n. Phase noise is further discussed in Section 4.2.

2.4 Demodulator

The demodulator obtains soft decision data from the received noisy and phase noise distorted complex-valued baseband signal, [9, Section 12], or, in other words, "estimates" the transmitted symbols. Additionally, the demodulator compensates for phase noise distortion by estimating or tracking phase noise processes. Estimation of phase noise can be performed jointly or separately with the estimation of the transmitted symbols. The soft decision data are either converted into hard decisions or fed into a channel decoder, provided that channel coding has been applied to the transmitted data [9, Section 14]. Different phase noise estimators, both joint and separate, are presented and discussed in Sections 4.3, 4.4, and 4.5.

CHAPTER 3

Wireless multi-antenna communication

This chapter provides an overview of multi-antenna communication in the form of multiple-input multiple-output (MIMO) wireless communication. As noted in [9, Section 20], multi-antenna communication equipment offers several advantages, such as increased area coverage, spatial diversity, and increased capacity. The MIMO systems discussed here are primarily aimed at improving capacity.

MIMO wireless communication is described in Section 3.1. Section 3.1.1 contains an introduction to a special case of MIMO, denoted line-of-sight MIMO (LOS-MIMO), which is part of the research in this thesis (Paper C).

3.1 MIMO wireless communication

A MIMO system with phase noise, as shown in Figure 3.1, models a single stream of information that is multiplexed into several streams. These multiplexed streams are transmitted over a wireless channel using several transmitter and receiver antennas affected by phase noise. A MIMO system, such as the one in Figure 3.1, enables *spatial multiplexing* of multiple data streams in parallel over the wireless channel, [9, Section 20.2].

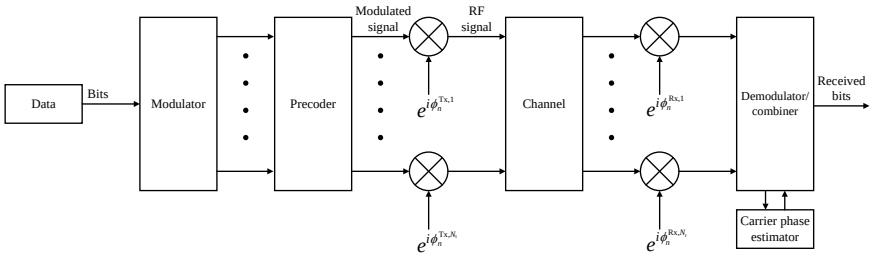

Figure 3.1: A MIMO model with phase noise.

The MIMO system in Figure 3.1 consists of a modulator that generates a number of parallel modulated streams, a precoder (described below), a number of transmitters affected by phase noise, a noisy multidimensional channel, a number of receivers affected by phase noise, and a demodulator (combiner) that takes a number of parallel streams as input. The different parts are described in Chapter 2.

The multiplexed streams transmitted from each antenna in a MIMO system are linearly combined (mixed) with the streams from the other antennas in the radio channel. The mixing of a memoryless channel with N_t transmitter antennas and N_r receiver antennas can be described by a channel matrix, [9, Section 20.2.3],

$$\boldsymbol{H}_{\mathrm{MIMO}} = \begin{pmatrix} h_{11} & h_{12} & \cdots & h_{1N_\mathrm{t}} \\ h_{21} & h_{22} & \cdots & h_{2N_\mathrm{t}} \\ \vdots & \vdots & \ddots & \vdots \\ h_{N_\mathrm{r}1} & h_{N_\mathrm{r}2} & \cdots & h_{N_\mathrm{r}N_\mathrm{t}} \end{pmatrix} , \tag{3.1}$$

where each element of the channel matrix corresponds to the complex scaling, or channel gain, from one transmitter antenna to one receiver antenna. If the channel corresponds to linearly independent combinations of the N_t ($N_\mathrm{r} \geq N_\mathrm{t}$) transmitted signals, they can be recovered through appropriate processing. As shown in [9, Section 20.2.5], for a system that has full knowledge of the channel state information (CSI) at both the transmitter and receiver, transmitter and receiver processing in the form of a transmitter *precoder* and a receiver *combiner* is often used to diagonalize the channel matrix. The resulting processed channel corresponds to multiple parallel streams (an equivalent diagonal channel). The precoder and combiner can, for example, be derived from the sin-

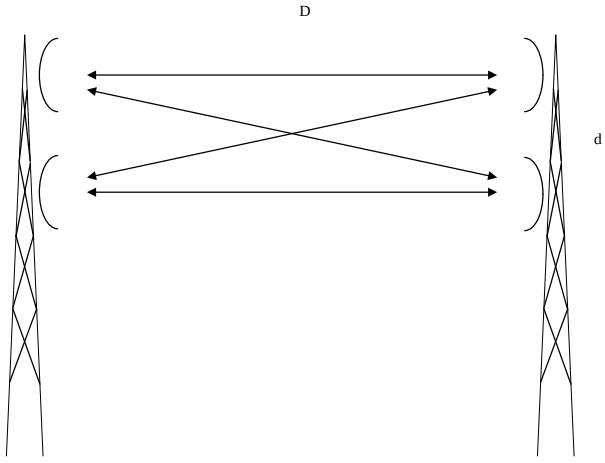

Figure 3.2: A 2×2 LOS-MIMO system.

gular value decomposition (SVD) of the channel matrix, $\boldsymbol{H}_{\text{MIMO}} = \boldsymbol{U}\boldsymbol{\Sigma}\boldsymbol{V}^{\text{H}}$, where the precoder is $\boldsymbol{V}$ and the combiner is $\boldsymbol{U}^{\text{H}}$.

An important special case of MIMO is multi-user MIMO (MU-MIMO), [9, Section 20.3]. In MU-MIMO, a cellular BS typically communicates with several UEs simultaneously, where the UEs generally do not cooperate, and all processing is performed at the BS. A variant of MU-MIMO is massive MIMO, in which the number of antennas at the BS increases by several orders of magnitude, [16]. Due to the massive number of BS antennas, massive MIMO has the potential to offer improved capacity while simultaneously reducing, for example, transmit power per antenna and decreasing hardware requirements for each antenna branch. Massive MIMO relies on the law of large numbers, which averages out noise, fading, and hardware imperfections.

3.1.1 The LOS-MIMO channel

A special case of MIMO, relevant to this thesis, is LOS-MIMO which is based on geometrical properties of the installed system, such as antenna positions

and the distance between transmitting and receiving antennas[1], as shown in Figure 3.2. The properties of the LOS-MIMO channel are discussed in this section. For a more detailed description, see Paper C.

In LOS, an orthogonal MIMO channel is achieved by mounting the antennas at the near-end and far-end in specific geometric configurations, i.e., specific distances between the antennas, which depend on the carrier frequency and the hop length. The elements of a LOS-MIMO channel matrix, $\boldsymbol{H}_{\text{LOS}}$, stem from the geometry of the LOS channels between the different antennas. As part of this thesis, uniform linear arrays[2] (ULAs) with a large distance, D, between transmitters and receivers compared to antenna separation, d, are considered, [17], where the carrier frequency is much higher than the bandwidth of the communication signal[3]. Different optimal antenna architectures for LOS-MIMO have been presented in the literature. ULAs are, for example, presented in [17], and a 3D approach is covered in [18].

Consider, for example, a 2×2 LOS-MIMO system (2 transmitters and 2 receivers), as shown in Figure 3.2. The channel matrix can be formulated as

$$\boldsymbol{H}_{\text{LOS}} \propto \begin{pmatrix} e^{\frac{i2\pi\sqrt{D^2}}{\lambda}} & e^{\frac{i2\pi\sqrt{D^2+d^2}}{\lambda}} \\ e^{\frac{i2\pi\sqrt{D^2+d^2}}{\lambda}} & e^{\frac{i2\pi\sqrt{D^2}}{\lambda}} \end{pmatrix} \approx \begin{pmatrix} e^{\frac{i2\pi D}{\lambda}} & e^{\frac{i2\pi(D+\frac{d^2}{2D})}{\lambda}} \\ e^{\frac{i2\pi(D+\frac{d^2}{2D})}{\lambda}} & e^{\frac{i2\pi D}{\lambda}} \end{pmatrix}, \tag{3.2}$$

where λ is the carrier wavelength. Each element in $\boldsymbol{H}_{\text{LOS}}$ represents a phase rotation based on the signal path distance between a transmitting and a receiving antenna. Optimal performance requires that the columns in $\boldsymbol{H}_{\text{LOS}}$ are orthogonal, which leads to the following optimal antenna separation, [17],

$$d_{\text{opt}} = \sqrt{\frac{\lambda D}{2}}. \tag{3.3}$$

Since D is large compared to the total antenna size (distance between the outermost antennas), $d_{\text{tot}} = (N-1)d$, the channel is dominated by LOS and the attenuation for all paths between any transmitter and receiver is approximately equal. Hence, the magnitudes of all elements in the channel matrix are modeled as being equal.

[1] Usually high gain antennas, such as parabolic antennas.

[2] Two-dimensional arrays are also feasible and the theory is similar.

[3] The LOS-MIMO channel matrix is often formulated using a continuous wave signal propagating between each transmitter and receiver. With sufficiently narrowband communication compared to the carrier frequency, the LOS-MIMO channel matrix is approximately valid over the complete bandwidth of the communication signal.

For installations with a low carrier frequency (large λ) and a long hop length (large D), the optimal antenna distance can become large. From (3.2), it is evident that a full-rank matrix can be achieved when $d < d_{\text{opt}}$. An installation with d below optimal is often referred to as suboptimal LOS-MIMO. However, as d approaches zero, the channel matrix reduces to rank 1, effectively becoming equivalent to a SISO channel.

CHAPTER 4

Pilot-based estimation of phase noise

Several aspects of pilot-based estimation of phase noise in wireless communication systems are presented in this chapter. The motivation for pilot-based phase noise estimation is discussed in Section 4.1. Two important phase noise models are introduced in Section 4.2. Finally, three pilot-based methods for phase noise estimation in wireless communication systems are explored in Sections 4.3, 4.4, and 4.5. These sections also demonstrate the effects of phase noise in different scenarios, including SISO SC, SISO OFDM, and LOS-MIMO.

4.1 Phase noise estimation based on payload or pilots

Phase noise estimation for a received wireless communication signal can be performed using pilots and/or the unknown payload, as mentioned in Section 1.1. This section provides a detailed motivation for pilot-based phase noise estimation by comparing methods based on pilots and payload.

As discussed in Section 1.1, the structure of the unknown payload, i.e., the modulation type, is normally known by the wireless communication equip-

ment. However, the *actual* content, i.e., the specific payload symbol being transmitted, is unknown. As a consequence, a phase estimator utilizing payload must treat the fact that the receiver observes noisy and distorted unknown transmitted symbols. Handling the uncertainties associated with the received payload is challenging, often leading to complex processing.

The transmission of known pilots is often used to estimate various unknown channel parameters [10]. However, known pilots introduce overhead because they are interleaved with (or added to) the payload. Since the pilots are known to the receiver and do not contribute to uncertainties, phase noise estimation based on pilots becomes less complex. Additionally, phase noise estimation based on the payload often relies on these pilots.

Estimation of the phase noise of the received signal can, depending on the type of modulated signal, be made in the frequency-domain or time-domain, using known pilots and/or the unknown payload. Phase noise is inherently a time-domain problem. The difference between the two types of modulated signals, SC and OFDM, primarily lies in how the Fourier transform is involved in modulation and demodulation. Since the processing differs, the two cases are treated separately below.

From a time-domain perspective, a powerful iterative phase noise estimation approach is presented in [12]. The proposed iterative algorithm suppresses the effects of symbol decision errors, but complexity and/or delay may become considerable because it relies on iterations over a channel decoder. Another powerful algorithm with trellis-based phase estimation is proposed in [19]. As with [12], the trellis-based approach suppresses the effects of symbol decision errors by iterating over a channel decoder, but the complexity and/or delay may become considerable. MIMO phase estimation is studied in [20], where an iterative expectation maximization (EM) algorithm that can incorporate channel decoding is proposed. Although several simplifications are introduced to balance complexity and performance, complexity and/or delay may still become considerable. MIMO phase estimation is also studied in [21], where a soft-input estimator is proposed. However, finding the maximum of the posterior probability density function (PDF) leads to an extensive search problem due to the unknown payload, and the resulting complexity and/or delay may become considerable, even if an error-correcting code is not involved.

From a frequency-domain perspective, the phase estimation of phase noise of an OFDM signal is analyzed in [22], where the estimation is performed using

decisions after an error-correcting code. Similar approaches can also be found in [23] and [24]. An iterative (using an error-correcting code) phase noise and channel estimation utilizing the geometrical properties of phase noise is presented in [14]. As with the time-domain perspective discussed above, the iterative approaches for OFDM may lead to significant complexity and/or delay.

Due to the complexity and delay problems related to payload uncertainties, phase estimation involving payload often becomes unfeasible. Instead, pilot-based estimation becomes an important alternative and, in many cases, the only practical option. However, as noted in Papers B and C, achieving close-to-optimal performance with pilot-based phase estimators can be surprisingly difficult.

4.2 Phase noise models

In model-based phase noise estimation, accurate phase noise modeling is crucial for achieving well-performing estimators, as demonstrated in [25] and [8]. Numerous models effectively capture the key aspects of phase noise effects. Both oscillator and phase noise modeling have been well studied, see, for example, [26] and [8, Section 3].

The bandwidth of phase noise is typically assumed to be much lower than that of the communication signal. It is commonly modeled as a time-discrete process with finite bandwidth, a widely accepted assumption in the literature (e.g., [12]–[15]).

This section introduces two different phase noise models used in the research covered by this thesis: the Wiener process, which models a free-running oscillator, and the first-order autoregressive process (AR(1)), which models a phase-locked loop (PLL).

4.2.1 The Wiener process

A widely used model for a free-running oscillator is the Wiener process, which effectively captures key properties of phase noise, specifically as a Gaussian random process with a variance that increases linearly over time [26]. The time-continuous Wiener phase noise process, as described in [27, Page 316],

evolves as

$$\theta(t) = u_0 + \int_0^t u(\tau)d\tau, \tag{4.1}$$

where u_0 is a uniform $[0\ 2\pi]$ variable. The process $u(t)$ is white and zero mean Gaussian with autocorrelation

$$\mathbb{E}[u(\tau)u(\tau+t)] = \sigma^2\delta(t), \tag{4.2}$$

where $\delta(t)$ is the Dirac delta function. While phase noise is inherently continuous, it is often modeled as a time-discrete process. The modeling of the time-continuous Wiener process as a time-discrete process is analyzed in [28], and the time-discrete Wiener phase noise process is described by

$$\theta_{n+1}^{\text{Wiener}} = \theta_n^{\text{Wiener}} + u_{n+1}, \tag{4.3}$$

where the innovation u_n is real, white and normal distributed, $\mathcal{N}(0, \sigma_u^2)$, and u_0 is uniform $[0\ 2\pi]$. The level of phase noise of a Wiener process is described by a single parameter, the variance of the innovation, σ_u^2.

As noted in [28], if the phase noise is not constant over the time span of the transmitted signal waveforms (e.g., a root-raised-cosine impulse), there will be inter-symbol interference (ISI) when using a matched filter in the receiver which does not consider phase noise[1]. In fact, the phase noise is not constant over the transmitted signal waveforms. However, if the phase variation is small enough, the resulting ISI distortion will be insignificant. According to [28], the time-discrete model is valid up to $\sigma_u^2 \lesssim 0.01$, which corresponds to strong phase noise.

4.2.2 The AR(1) process

A common approach when designing oscillators is to use a PLL that is locked to a reference oscillator. A typical reference source is a crystal oscillator, which generally exhibits low phase noise[2]. As the Wiener process is non-stationary, it is not suitable for modeling PLLs, and some modifications are necessary

[1] Commonly, the receiver filtering in wireless communication systems does not consider phase noise.

[2] Crystal oscillators generally have a limited or fixed frequency tuning range and a high Q-factor, resulting in low phase noise that is often dominated by a white noise floor [7].

to achieve a relevant stationary process[3]. As shown in, for example, [29], the phase noise of a PLL has limited variance and is wide-sense stationary (WSS), see [11, Note 25.4.3]. The phase noise power spectral density (PSD) of a properly tuned PLL is shown, for example, in [29, Figure 1b)].

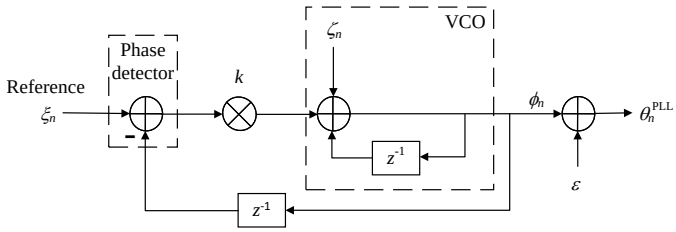

Figure 4.1: A time-discrete PLL model with a Wiener process VCO.

Since PLLs operate as feedback control systems [30], a feedback control approach is adopted to formulate a simple yet effective time-discrete PLL model. A first-order, time-discrete PLL model, using a Wiener process to model a voltage-controlled oscillator (VCO), is shown in Figure 4.1. There are two sources of independent zero mean white and normal distributed noise, namely reference noise (from the phase detector and reference oscillator), ξ_n, with variance σ_ξ^2, and VCO innovation noise, ζ_n, with variance σ_ζ^2. Additionally, there is a deterministic uniform $[0\ 2\pi]$ phase uncertainty, ε, in the PLL to model an actual analog design.

The two transfer functions for the reference to output, ξ_n to θ_n^{PLL}, and the VCO to output, ζ_n to θ_n^{PLL}, are

$$H_{\mathrm{Ref}}(z) = \frac{\frac{k}{1-z^{-1}}}{1+\frac{kz^{-1}}{1-z^{-1}}} = \frac{k}{1-(1-k)z^{-1}}, \tag{4.4}$$

and

$$H_{\mathrm{VCO}}(z) = \frac{\frac{1}{1-z^{-1}}}{1+\frac{kz^{-1}}{1-z^{-1}}} = \frac{1}{1-(1-k)z^{-1}}, \tag{4.5}$$

[3]As the PLL is locked to a reference which is not free of phase noise, it is not, strictly speaking, stationary. However, the phase noise of the reference crystal oscillator in the PLL is often insignificant compared to the phase noise of the VCO used in the PLL, and *stationary* is therefore a valid approximation.

where the loop gain k is $0 \leq k \leq 1$. The optimal k, which depends on the variance of the reference and VCO innovation, is discussed further below. Using $k = 0$ results in a free-running oscillator modeled as a Wiener process (no PLL control), and using $k = 1$ results in white phase noise characterized by the reference noise and the innovation of the VCO. With $0 < k \leq 1$, the PLL is stationary with mean ε. The corresponding PSD of the resulting phase noise is

$$\begin{aligned} P_\theta(f) &= \frac{2}{f_\mathrm{s}} \left(\sigma_\xi^2 |H_\mathrm{Ref}(e^{i2\pi f/f_\mathrm{s}})|^2 + \sigma_\zeta^2 |H_\mathrm{VCO}(e^{i2\pi f/f_\mathrm{s}})|^2 \right) \\ &= \frac{2}{f_\mathrm{s}} \frac{k^2\sigma_\xi^2 + \sigma_\zeta^2}{\left|1 - (1-k)e^{-i2\pi f/f_\mathrm{s}}\right|^2}, \end{aligned} \tag{4.6}$$

where f_s is the sample rate.

Looking at (4.4), (4.5), and (4.6), it is evident that the PLL can be modeled as an AR(1) process [31, App. 1.2.4] with mean ε. The resulting phase noise model becomes

$$\theta_n^\mathrm{PLL} = \phi_n + \varepsilon, \tag{4.7}$$

where ϕ_n is an AR(1) process formulated as

$$\phi_{n+1} = a\phi_n + u_{n+1}. \tag{4.8}$$

The forgetting factor, or AR(1) coefficient, is $a = 1-k$, and the innovation, u_n, is $\mathcal{N}(0, \sigma_u^2)$, where $\sigma_u^2 = \sigma_\zeta^2 + k^2\sigma_\xi^2$. It should be noted that the AR(1) process PLL model has been proposed in many papers, such as [30] and [32]. Since the symbol rates (bandwidth of the wireless communication signal) within the research covered by this thesis are moderate, and the noise floor of oscillators is typically small[4], the PLL model noise floor is omitted.

[4]The noise floor integrated over the bandwidth of the communication signal is small.

By reformulating the AR(1) model, (4.8), into a single sum

$$\begin{aligned}
\phi_n &= a\underbrace{\left(a\underbrace{\left(a(\cdots)+u_{n-2}\right)}_{\phi_{n-2}}+u_{n-1}\right)}_{\phi_{n-1}}+u_n \\
&= \sum_{k=0}^{n-1} a^{n-k}u_k + u_n \\
&= \sum_{k=0}^{n} a^{n-k}u_k \\
&= \sum_{l=0}^{n} a^{l}u_{n-l}, \qquad (4.9)
\end{aligned}$$

the total variance of the PLL, for $a < 1$, asymptotically becomes

$$\begin{aligned}
\sigma_\phi^2 &= \mathbb{E}\left[\phi_n^2\right] \\
&= \mathbb{E}\left[\left(\sum_{l=0}^{n} a^l u_{n-l}\right)\left(\sum_{l=0}^{n} a^l u_{n-l}\right)\right] \\
&= \sigma_u^2 \sum_{l=0}^{n} a^{2l} \\
&\to \frac{\sigma_u^2}{1-a^2},\ n \to \infty, \qquad (4.10)
\end{aligned}$$

since the innovations are independent. To conclude, the optimal k for the PLL in Figure 4.1 can be found by minimizing

$$\sigma_\phi^2 = \frac{\sigma_\zeta^2 + k^2\sigma_\xi^2}{1-(1-k)^2}. \qquad (4.11)$$

A PLL model according to (4.7) can, for example, be characterized by the 3 dB bandwidth, $f_{3\text{dB}}$, and innovation variance, σ_u^2. The factor a can be calculated from $f_{3\text{dB}}$ for a given sample rate, f_s, using the PSD, (4.6). Consequently, the factor a is one of the solutions to the second order equation

$$\frac{1}{|1-ae^{-i2\pi f_{3\text{dB}}/f_s}|^2} = \frac{0.5}{|1-a|^2}, \qquad (4.12)$$

where the root of interest satisfies $0 \le a < 1$.

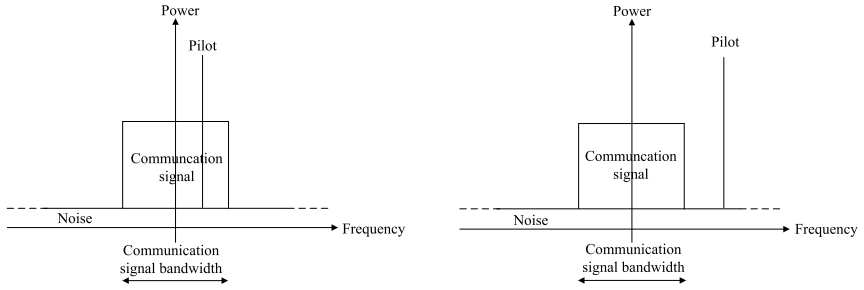

(a) In-band CW pilot **(b)** Out-of-band CW pilot

Figure 4.2: Power spectrums of communication signals with CW pilots within and outside the bandwidth of the signal.

Comparing Figures 4.3 (a) and (b) in Section 4.3 below, phase noise distortion is more pronounced in the Wiener model than in the AR(1) model, because the Wiener model is non-stationary. However, the AR(1) coefficient a approaches one even for relatively high PLL bandwidths $f_{3\text{dB}}$. For instance, setting $f_{3\text{dB}} = f_s/1000$ in (4.12) results in $a \approx 0.994$. When a is close to one, an estimator may assume $a = 1$ without significantly penalizing estimation performance (see Paper C). Although oscillators in wireless communication systems are typically implemented as PLLs, the Wiener process model is often used as a practical approximation for formulating phase estimators.

4.3 Phase noise estimation using continuous-wave pilots

This section presents research on phase noise estimation using continuous-wave pilots (CW pilots). Additionally, Section 4.3.1 shows the effect of phase noise distortion in a SC system.

According to Paper A, the observed received, phase noise distorted, signal can be formulated as

$$\begin{aligned} y'_n &= \underbrace{\sqrt{1-\beta^2}x_n e^{i(\theta_n^{(\text{Tx})}+\theta_n^{(\text{Rx})})}}_{\text{communication signal}} + \underbrace{\beta\sigma_x e^{i(f_{CW}n+\theta_n^{(\text{Tx})}+\theta_n^{(\text{Rx})})}}_{\text{CW pilot}} + \underbrace{u'_n e^{i\theta_n^{(\text{Rx})}}}_{\text{AWGN}} \\ &= \sqrt{1-\beta^2}x_n e^{i\theta_n} + \beta\sigma_x e^{i(\theta_n + f_{\text{CW}}n)} + u_n. \end{aligned} \tag{4.13}$$

The transmitted power, σ_x^2, is shared between a CW pilot at a known frequency, f_{CW}, and the communication signal, x_n, using the parameter β. The CW pilot can either reside within the bandwidth, *in-band*, or outside the bandwidth of the communication signal, *out-of-band*, as is illustrated in Figure 4.2. The communication signal is unknown, rotation-invariant, complex, and normal distributed, i.e., $x_n \sim \mathcal{CN}(0, \sigma_x^2)$, and is white over its Nyquist bandwidth. The up-conversion contributes with a transmitter phase noise $\theta_n^{(\text{Tx})}$, and the down-conversion contributes with a receiver phase noise $\theta_n^{(\text{Rx})}$. These two phase noise contributions are independent of each other and are modeled as Wiener phase noise (see Section 4.2.1). The two phase noises are summed into one total phase noise contribution $\theta_n = \theta_n^{(\text{Tx})} + \theta_n^{(\text{Rx})}$. The receiver also contributes with a rotation-invariant complex AWGN, u'_n.

By applying an ideal low-pass filter, h, that suppresses any noise and communication signal contributions outside the relevant bandwidth of the CW pilot, and compensating for the known frequency error, the resulting signal which can be used for estimation becomes

$$\begin{aligned} y_n &= h * \frac{1}{\sigma_x \beta} y'_n e^{-i f_{\text{CW}} n} \\ &= e^{i\theta_n} + \underbrace{h * \frac{1}{\sigma_x \beta} \left(\sqrt{1-\beta^2} x_n e^{i(\theta_n - f_{\text{CW}} n)} + u_n e^{-i f_{\text{CW}} n} \right)}_{\text{Gaussian noise, } w_n} \\ &\triangleq e^{i\theta_n} + w_n. \end{aligned} \tag{4.14}$$

The filtered noise, w_n, is Gaussian and depends on the in-band and out-of-band scenarios. The resulting estimator model in (4.14) represents a CW tone in noise, which is affected by phase noise.

Looking at (4.13) and (4.14), there are two problems, estimating the phase noise and determining an optimal signal to pilot power ratio (SPR), such as the optimal β that maximizes SNDR. One approach is to use a filter with an optimal bandwidth for estimating the phase noise to maximize SNDR, i.e., filtering the phasor in (4.14), as proposed in [33]. Additionally, since (4.14) can be interpreted as a SC system with time-interleaved pilots, a Wiener-type of filter can be formulated to estimate the phase noise, as shown in [13]. A more comprehensive approach involves estimating the phase noise using a filter with an optimal bandwidth, while simultaneously finding the optimal

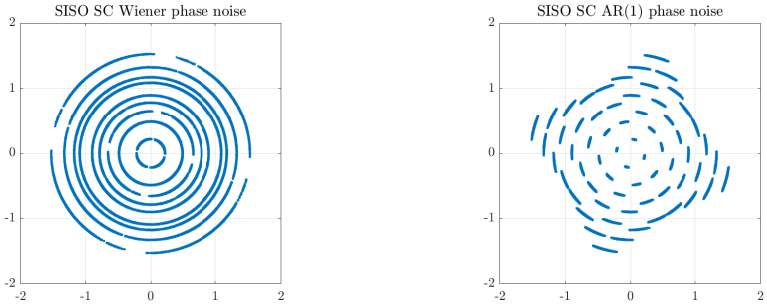

(a) Wiener phase noise **(b)** AR(1) phase noise

Figure 4.3: SISO 64-QAM SC signals affected by different phase noises, with an SNR of 50 dB, a phase noise innovation variance of 10^{-5}, and an AR(1) coefficient of $a = 0.999$.

SPR[5], as discussed in [34], [35], and [36].

Earlier papers related to using a CW pilot for estimating phase noise of a communication signal have focused on the practical and empirical aspects of phase estimation. Instead, Paper A provides a comprehensive foundation for the theory and practice of optimal phase estimation using CW pilot tones. The derivation of the proposed *improved estimator* in Paper A is concise and straightforward. It achieves near-optimal performance across a wide range of phase noise levels and SNR values, and it can easily be adapted for different phase noise models by modifying the phase noise covariance matrix. Notably, the resulting estimator can be implemented using analog processing, allowing for phase estimation close to the antenna. Although the maximum likelihood (ML) derivation follows a classical estimation theory approach, the estimator is, in fact, the minimum mean square error (MMSE) estimator, since the prior is uniform over $[0\ 2\pi]$. In addition, the optimal SPR that maximizes the SNDR is presented for the in-band and out-of-band cases.

[5]Maximizing SNDR, for example, as a function of estimation filter bandwidth and SPR, typically reduces to an extensive search problem.

4.3.1 SC affected by phase noise

An observed SC signal can, from (4.13) with $\beta = 0$, be formulated as

$$y_n = x_n e^{i\theta_n} + u_n, \tag{4.15}$$

where x_n consists of 64-QAM symbols in this example. The effects of the two different phase noises, Wiener and AR(1), are illustrated in Figure 4.3 (a) and (b) for a SISO 64-QAM SC simulation. The SNR is 50 dB, the phase noise innovation variance is 10^{-5}, and the AR(1) coefficient a is 0.999. Even though the realization of the innovation noise is the same for both phase noises in this example, the phase error is larger for the Wiener phase noise compared to that of AR(1), and the difference increases as the simulation batch length grows. This is expected, as Wiener phase noise is non-stationary, while AR(1) is stationary with a mean of ε.

4.4 Phase noise estimation in OFDM systems

This section presents research related to pilot-based estimation of phase noise for OFDM systems. Furthermore, the phase noise distortion of an OFDM signal is shown in Section 4.4.1.

Paper B examines a system in which known pilots are embedded as designated subcarriers within an OFDM signal, transmitted over a frequency-selective channel affected by phase noise. According to Paper B, the received signal can be formulated as

$$\boldsymbol{y} = \underbrace{\boldsymbol{F}\overbrace{e^{i\boldsymbol{\Theta}_{\mathrm{Rx}}}}^{\text{time domain}}\boldsymbol{F}^{-1}}_{\substack{\text{cyclic shifted}\\ \text{DFT of phasor}}}\boldsymbol{H}\underbrace{\boldsymbol{F}\overbrace{e^{i\boldsymbol{\Theta}_{\mathrm{Tx}}}}^{\text{time domain}}\boldsymbol{F}^{-1}}_{\substack{\text{cyclic shifted}\\ \text{DFT of phasor}}}\boldsymbol{x} + \boldsymbol{e} + \boldsymbol{w}, \tag{4.16}$$

where the AWGN, $\boldsymbol{w}$, is $\mathcal{CN}(\boldsymbol{0}, \sigma_w^2\boldsymbol{I})$. The vector $\boldsymbol{x}$ contains independent QAM payload data symbols and a sparse number of known constant-amplitude pilots at known positions (subcarriers). The matrix $\boldsymbol{F}$ is the discrete Fourier transform (DFT). A cyclic prefix (CP) is added to the transmitted time-domain version of the signal, [9, Section 19.4.1], and the resulting cyclic channel filtering can be modeled as a diagonal channel matrix, $\boldsymbol{H} = \mathrm{diag}\{\boldsymbol{Fh}\}$, where $\mathrm{diag}\{\boldsymbol{a}\}$ is a diagonal matrix containing the vector $\boldsymbol{a}$. The vector $\boldsymbol{e}$ is a

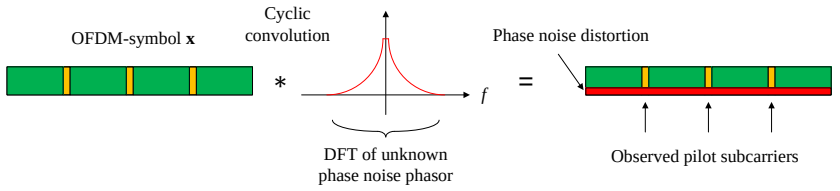

Figure 4.4: An illustration of a received phase noise-distorted OFDM signal, where the DFT of the phase noise phasor circularly convolves with the frequency-domain representation of the OFDM symbol. The known pilot subcarriers are marked in yellow, the unknown payload in green, and the resulting phase noise distortion floor in red.

(small) term that corresponds to the modeling error related to the transmitter phase noise not being cyclic over the OFDM symbol. The phase noise matrix, $\mathbf{\Theta}$, is diagonal and contains the phase noise process vector variable, and $e^{i\mathbf{\Theta}}$ is defined as a diagonal element-wise exponential resulting in an appropriate phasor matrix. The transmitter and receiver phase noise are modeled as Wiener phase noise (see 4.2.1).

The symbols are mapped on the subcarriers of the OFDM symbol (frequency-domain) and the phase noise rotates (multiplies) the time-domain representation of the OFDM symbol. This means that the Fourier transform of the phase noise convolves (filters) the frequency-domain representation of the OFDM symbol, [11, Section 6.2], as highlighted in (4.16). The phase noise distortion is visualized in Figure 4.4 for a memoryless unity-gain channel. The goal is to estimate the phase noise using the known pilots, without relying on hard or soft decisions. However, using only known pilots (marked in yellow in Figure 4.4) with an unknown payload (marked in green) makes estimation challenging, as the payload is essentially strong noise for the estimator. The phase noise distortion floor (marked in red) is the convolution of the OFDM symbol containing IID payload (or pilots) and the DFT of the phase noise phasor. Even though the phase noise floor is present at all subcarriers, it is only possible to observe the distortion at pilot positions. However, the convolution from the unknown strong payload surrounding the pilots dominates the observation.

There are different possibilities to approach the problem of pilot-based es-

timation of phase noise in a wireless OFDM communication signal. To partly avoid the issue of the convolution becoming dominated by the payload, pilots can be allocated next to each other (i.e., frequency-consecutive) in the OFDM symbol. By using frequency-consecutive pilots, an MMSE estimate can be formulated, minimizing the phase error over a larger bandwidth, [37] and [38]. However, consecutive pilots can be disadvantageous if, for example, a selective channel severely attenuates the frequency range covered by the consecutive pilots. To allow for distributed pilots, the sum of the squared errors of the pilots can be minimized with respect to the phase noise (instead of, for example, minimizing the error of the phase noise statistically as the MMSE), i.e., to minimize $(\boldsymbol{y}_{\text{pilot}} - \boldsymbol{x}_{\text{pilot}})^{\text{H}}(\boldsymbol{y}_{\text{pilot}} - \boldsymbol{x}_{\text{pilot}})$ with respect to the phase noise, where $\boldsymbol{x}_{\text{pilot}}$ and $\boldsymbol{y}_{\text{pilot}}$ corresponds to the pilot subcarriers of the transmitted and received OFDM symbol. The resulting estimator is usually of least squares (LS) type without incorporating phase noise statistics, [15] and [39]. Geometry-preserving estimation means, according to [39], that the estimated phase noise phasor, $\widehat{e^{i\boldsymbol{\Theta}}}$, must fulfill the requirement that the columns of the matrix $\boldsymbol{F}e^{i\boldsymbol{\Theta}}\boldsymbol{F}^{-1}$ are orthogonal. Using a geometry-preserving phase noise model combined with a constrained version of LS results in close to optimal performance, [39]. However, due to the constrained LS, the complexity becomes significant.

As shown in Paper B, it is possible to formulate an MMSE estimate of phase noise, which is close to optimal over a large dynamic range of phase noise levels and SNR, without any constraints on how pilots are allocated across subcarriers. The method proposed in Paper B also has significantly lower complexity compared to other optimal solutions in the literature. An increasing pilot-rate decreases the distortion related to the phase noise. However, a higher pilot-rate also reduces the payload rate since the overhead increases. Regarding the balance between distortion and pilot overhead, the pilot-rate maximizing the payload rate is presented. Additionally, it is shown that phase noise can be approximated using principal component analysis (PCA) [40], where the number of estimated parameters can be significantly reduced with only a minor impact on the accuracy of the estimated phase noise. Furthermore, it is demonstrated that a system with both transmitter and receiver phase noise can be approximated as having receiver-only phase noise if certain conditions are met[6].

[6] A channel that is not "too selective" and phase noise that is not too dominant.

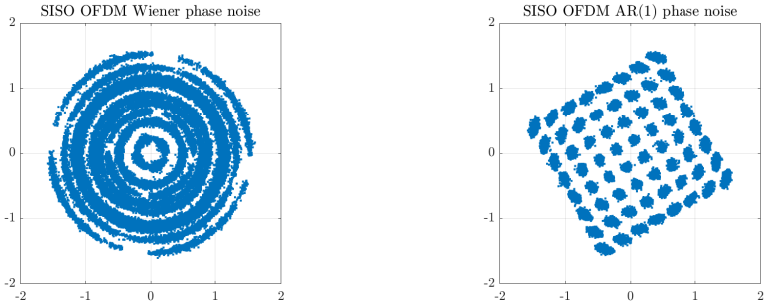

(a) Wiener phase noise **(b)** AR(1) phase noise

Figure 4.5: SISO 64-QAM OFDM signals affected by different phase noises, with an SNR of 50 dB, a phase noise innovation variance of 10^{-5}, and an AR(1) coefficient of $a = 0.999$.

4.4.1 OFDM affected by phase noise

By factoring out the average phase in the form of phasors of the transmitter and receiver phase noise, $e^{i\bar{\theta}^{\mathrm{Tx}}}$ and $e^{i\bar{\theta}^{\mathrm{Rx}}}$, from (4.16), the observed signal vector can be formulated as

$$\begin{aligned}\boldsymbol{y} &= \boldsymbol{F}e^{i\bar{\theta}^{\mathrm{Rx}}}e^{-i\bar{\theta}^{\mathrm{Rx}}}e^{i\boldsymbol{\Theta}_{\mathrm{Rx}}}\boldsymbol{F}^{\text{-}1}\boldsymbol{H}e^{i\bar{\theta}^{\mathrm{Tx}}}e^{-i\bar{\theta}^{\mathrm{Tx}}}\boldsymbol{F}e^{i\boldsymbol{\Theta}_{\mathrm{Tx}}}\boldsymbol{F}^{\text{-}1}\boldsymbol{x} + \boldsymbol{e} + \boldsymbol{w} \\ &= \underbrace{e^{i(\bar{\theta}^{\mathrm{Tx}}+\bar{\theta}^{\mathrm{Rx}})}}_{\text{CPE}} \underbrace{\underbrace{\boldsymbol{F}e^{-i\bar{\theta}^{\mathrm{Rx}}}e^{i\boldsymbol{\Theta}_{\mathrm{Rx}}}\boldsymbol{F}^{\text{-}1}}_{\text{ICI Rx}}\boldsymbol{H}\underbrace{\boldsymbol{F}e^{-i\bar{\theta}^{\mathrm{Tx}}}e^{i\boldsymbol{\Theta}_{\mathrm{Tx}}}\boldsymbol{F}^{\text{-}1}}_{\text{ICI Tx}}}_{\text{nondiagonal matrix}}\boldsymbol{x} + \boldsymbol{e} + \boldsymbol{w},\end{aligned} \tag{4.17}$$

where the matrices $\boldsymbol{F}e^{-i\bar{\theta}^{\mathrm{Rx}}}e^{i\boldsymbol{\Theta}_{\mathrm{Rx}}}\boldsymbol{F}^{\text{-}1}$ and $\boldsymbol{F}e^{-i\bar{\theta}^{\mathrm{Tx}}}e^{i\boldsymbol{\Theta}_{\mathrm{Tx}}}\boldsymbol{F}^{\text{-}1}$ are nondiagonal. Hence, even though $\boldsymbol{H}$ is diagonal, the resulting transmission of $\boldsymbol{x}$ is based on a nondiagonal matrix. In (4.17), the phase noise distortion is separated into a common phase error (CPE) for all subcarriers of an OFDM symbol (the DC part of the Fourier transform of the phase noise phasor) and an inter-carrier interference (ICI) between the different subcarriers of the OFDM symbol (the non-DC parts of the Fourier transform of the phase noise phasor).

The phase noise distortion of a SISO 64-QAM OFDM signal with 1024 subcarriers is shown in Figure 4.5 for Wiener and AR(1) phase noise (several OFDM symbols). The SNR is 50 dB, the phase noise innovation variance

is 10^{-5}, and the AR(1) coefficient a is 0.999. The effect of the CPE can be understood by comparing the average phase noise rotation of the received signal in Figure 4.3 (b) with that in Figure 4.5 (b). Here, ε is the same in both simulations, and therefore the average rotation is identical. The effect of ICI can also be understood by comparing Figure 4.5 (b) with Figure 4.3 (b), where the ICI part of the phase noise appears as an additive noise affecting both the amplitude and phase of the OFDM signal, while all phase noise, in contrast, results in a rotation of the SC signal.

4.5 Phase noise estimation in LOS-MIMO systems

This section presents research related to pilot-based estimation of phase noise for LOS-MIMO systems. Additionally, the phase noise distortion for a LOS-MIMO system is shown in Section 4.5.1.

Paper C examines a system in which known pilots are periodically interleaved in an $N \times N$ LOS-MIMO wireless communication signal affected by phase noise. According to Paper C, the received signal can be formulated as

$$\boldsymbol{y}_n = e^{i\boldsymbol{\Theta}_n^{(\mathrm{Rx})}} \boldsymbol{H}_{\mathrm{LOS}}\, e^{i\boldsymbol{\Theta}_n^{(\mathrm{Tx})}} \boldsymbol{T}\boldsymbol{s}_n + \boldsymbol{w}_n, \tag{4.18}$$

where the channel, $\boldsymbol{H}_{\mathrm{LOS}}$, is known. The transmitted information vector, $\boldsymbol{s}_n$, of length N, contains payload in the form of independent, rotation-invariant complex Gaussian samples, i.e., $\boldsymbol{s}_n \sim \mathcal{CN}(\boldsymbol{0}, \boldsymbol{Q}_s)$, where the power allocation, $\boldsymbol{Q}_s = \mathbb{E}[\boldsymbol{s}_n \boldsymbol{s}_n^{\mathrm{H}}]$, of $\boldsymbol{s}_n$ is chosen according to the channel conditions. A zero diagonal element of $\boldsymbol{Q}_s$ corresponds to an unused stream, and the actual (used) number of streams may be less than N. The trace of the precoded signal covariance, $\boldsymbol{Q}_x = \boldsymbol{T}\boldsymbol{Q}_s\boldsymbol{T}^{\mathrm{H}}$, represents the total transmitted power, σ_x^2. Periodically, $\boldsymbol{s}_n$ also contains known constant-amplitude pilots with power allocation $\boldsymbol{Q}_s$, which are independent of the payload. Hence, the pilots are precoded with the same precoder as the payload. The diagonal phasor matrices, $e^{i\boldsymbol{\Theta}_n^{(\mathrm{Tx})}}$ and $e^{i\boldsymbol{\Theta}_n^{(\mathrm{Rx})}}$, contain the N phase noises of the transmitter and the N phase noises of the receiver. The phase noises for all transmitters and receivers are independent and are modeled according to Section 4.2.2, i.e., AR(1) phase noise. All receivers have independent Gaussian, rotation-invariant complex AWGN contributions, i.e., $\boldsymbol{w}_n \sim \mathcal{CN}(\boldsymbol{0}, \sigma_w^2 \boldsymbol{I})$.

As illustrated in Figure 4.6, each received signal $y_n^{(k)}$ contains a linear combination of all transmitted precoded symbols, $x_n^{(1)}$ to $x_n^{(N)}$, affected by phase

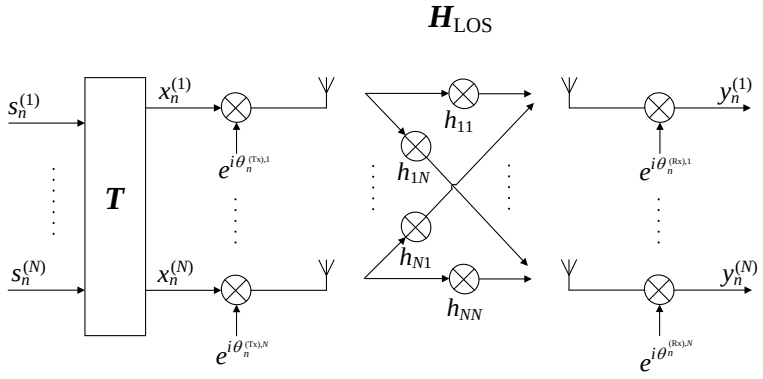

Figure 4.6: A LOS-MIMO signal model with phase noise distortion.

noise and is formulated as

$$y_n^{(k)} = e^{i\theta_n^{(\text{Rx}),k}} \left(h_{k1} x_n^{(1)} e^{i\theta_n^{(\text{Tx}),1}} + \cdots + h_{kN} x_n^{(N)} e^{i\theta_n^{(\text{Tx}),N}} \right) + w_n^{(k)}. \tag{4.19}$$

The main problem here is to estimate the payload part of $x_n^{(1)}$ to $x_n^{(N)}$ using known periodic pilots, in the presence of phase noise, under the assumption that the channel is known. The model is inherently nonlinear, both because the phase noise phasors are a nonlinear function of the unknown phase noise, and because the unknown payload multiplies the unknown phase noises.

Blind phase synchronization is studied in [41], where a phase offset estimation algorithm based on space-time block codes (STBC) for $2 \times N$ MIMO systems is presented. A special periodic pilot pattern for phase noise estimation is used in [42], where a pilot is transmitted on one antenna while all other antennas are muted. The overhead increases with the number of transmit antennas in the MIMO system, but each received signal becomes a function of one transmitter phase noise and one receiver phase noise, see (4.19). Assuming that the phase noise is small, similarly to the SISO case in [13], [42] approximates the phase noise exponentials using a first-order Taylor expansion. From the resulting linear relationships, a Wiener filter is formulated to jointly estimate all phase noises. While [42] formulated a Wiener filter interpolation between pilots, linear interpolation is evaluated in [43]. Instead, using extended Kalman filtering (EKF), as shown in [31, Section 13.7] and

[44], it is possible to estimate all phase noise processes jointly using pilots transmitted simultaneously on all transmitters. The EKF also estimates the phase noise between the pilots according to the phase noise model. Such an estimator corresponds to a pilot-based version of [21]. From the estimated phase, the transmitted payload can be estimated following the approach in [31, Eq. (15.64)].

By evaluating and reformulating (4.18), a novel linear pilot-based MMSE estimator is presented in Paper C. This estimator jointly estimates the payload, $\boldsymbol{s}_n$, and the phase noises, $\boldsymbol{\Theta}_n^{(\mathrm{Tx})}$ and $\boldsymbol{\Theta}_n^{(\mathrm{Rx})}$. In this method, pilots are transmitted periodically without any requirements for grouping or "special" pilot patterns. Since phase noise is a multiplicative distortion, performance depends on the power allocation, $\boldsymbol{Q}_s$, of the transmitted signal. Standard water-filling [45] may not achieve the maximum rate when the phase noise is significant. Consequently, an alternative power allocation strategy is evaluated, offering improved performance for channels with a high condition number at high phase noise levels. Similarly to the pilot-based estimation of phase noise for OFDM in Section 4.4, the optimal pilot rate that maximizes the payload rate for LOS-MIMO is presented.

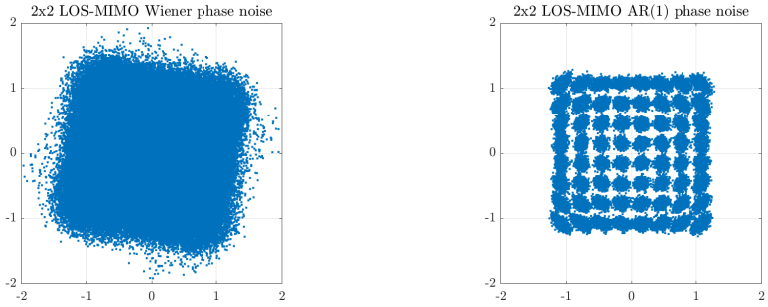

(a) Wiener phase noise

(b) AR(1) phase noise

Figure 4.7: 2×2 LOS-MIMO 64-QAM signals (one of the streams) affected by different phase noises. The SNR is 50 dB, the phase noise innovation variance is 10^{-5}, and an AR(1) coefficient of $a = 0.999$.

4.5.1 LOS-MIMO affected by phase noise

Figure 4.7 illustrates the phase noise distortion in a 2×2 LOS-MIMO 64-QAM wireless communication system with optimal antenna spacing, as described in (3.2) and (3.3). The figure shows one of the two transmitted symbol streams under both Wiener and AR(1) phase noise models. The SNR is 50 dB, the phase noise innovation variance is 10^{-5}, and the AR(1) coefficient a is 0.999. To resolve channel cross-talk, additional processing can, as mentioned in Section 3.1, be introduced. According to (4.18), the received signal is described by

$$\boldsymbol{y}_n = \boldsymbol{U}^{\mathrm{H}} e^{-i\boldsymbol{\Theta}_0^{(\mathrm{Rx})}} e^{i\boldsymbol{\Theta}_n^{(\mathrm{Rx})}} \boldsymbol{H}_{\mathrm{LOS}}\, e^{i\boldsymbol{\Theta}_n^{(\mathrm{Tx})}} e^{-i\boldsymbol{\Theta}_0^{(\mathrm{Tx})}} \boldsymbol{V}\boldsymbol{s}_n + \boldsymbol{U}^{\mathrm{H}}\boldsymbol{w}_n, \tag{4.20}$$

where the additional matrices, $\boldsymbol{U}$ and $\boldsymbol{V}$, are the orthonormal left and right singular vector matrices from the singular value decomposition of the channel, $\boldsymbol{H}_{\mathrm{LOS}} = \boldsymbol{U}\boldsymbol{\Sigma}\boldsymbol{V}^{\mathrm{H}}$. As described in Section 3.1, the pre- and post-multiplication with $\boldsymbol{V}$ and $\boldsymbol{U}^{\mathrm{H}}$ for a phase noise-free scenario leads to $\boldsymbol{U}^{\mathrm{H}}\boldsymbol{H}_{\mathrm{LOS}}\boldsymbol{V} = \boldsymbol{U}^{\mathrm{H}}\boldsymbol{U}\boldsymbol{\Sigma}\boldsymbol{V}^{\mathrm{H}}\boldsymbol{V} = \boldsymbol{\Sigma}$, where $\boldsymbol{\Sigma}$ is a diagonal matrix containing the singular values of $\boldsymbol{H}_{\mathrm{LOS}}$. For a LOS-MIMO channel with an optimal antenna configuration, the singular values are all equal. The noise vectors $\boldsymbol{U}^{\mathrm{H}}\boldsymbol{w}_n$ and $\boldsymbol{w}_n$ have the same statistical properties. Without loss of generality, the initial phases of all phase noises, $\boldsymbol{\Theta}_0^{(\mathrm{Tx})}$ and $\boldsymbol{\Theta}_0^{(\mathrm{Rx})}$, are assumed to be known here and

are used to normalize the transmitter and receiver phase noise with $e^{-i\boldsymbol{\Theta}_0^{(\mathrm{Tx})}}$ and $e^{-i\boldsymbol{\Theta}_0^{(\mathrm{Rx})}}$. As a result, for the AR(1) phase noise case, the average rotation of the received and compensated signal is zero.

The phase noise distortion observed in Figure 4.7 consists of two main effects: phase rotation and cross-talk. The cross-talk can be understood from the fact that

$$\boldsymbol{y}_n = \underbrace{\underbrace{\boldsymbol{U}^{\mathrm{H}} e^{-i\boldsymbol{\Theta}_0^{(\mathrm{Rx})}} e^{i\boldsymbol{\Theta}_n^{(\mathrm{Rx})}} \boldsymbol{U}}_{\substack{\text{nondiagonal}\\ \text{matrix}}} \boldsymbol{\Sigma} \underbrace{\boldsymbol{V}^{\mathrm{H}} e^{i\boldsymbol{\Theta}_n^{(\mathrm{Tx})}} e^{-i\boldsymbol{\Theta}_0^{(\mathrm{Tx})}} \boldsymbol{V}}_{\substack{\text{nondiagonal}\\ \text{matrix}}}}_{\substack{\text{nondiagonal}\\ \text{matrix}}} \boldsymbol{s}_n + \boldsymbol{w}_n, \tag{4.21}$$

contains non-diagonal matrices, i.e., $\boldsymbol{U}^{\mathrm{H}} e^{-i\boldsymbol{\Theta}_0^{(\mathrm{Rx})}} e^{i\boldsymbol{\Theta}_n^{(\mathrm{Rx})}} \boldsymbol{U}$ and $\boldsymbol{V}^{\mathrm{H}} e^{i\boldsymbol{\Theta}_n^{(\mathrm{Tx})}} e^{-i\boldsymbol{\Theta}_0^{(\mathrm{Tx})}} \boldsymbol{V}$ become nondiagonal due to the phase noise. As a result, there is cross-talk between the transmitted symbol streams. Looking at (4.17) and (4.21), the phase noise distortion of SISO OFDM and LOS-MIMO is similar, with rotation and cross-talk (between streams or subcarriers). The main difference lies in how the phase noise matrices are defined. These similarities are also evident when comparing Figures 4.5 and 4.7.

CHAPTER 5

Summary of included papers

This chapter provides a brief summary of the included papers.

5.1 Paper A

Björn Gävert, Thomas Eriksson
Estimation of Phase Noise Based on In-Band and Out-of-Band Frequency Domain Pilots
IEEE Transactions on Communications,
Volume: 70, Issue: 7, July 2022

A communication model incorporating a pilot tone for phase estimation is proposed, where the pilot tone can be placed either within or outside the bandwidth of the communication signal. Several estimators for phase noise estimation using the pilot tone are evaluated. Additionally, the optimal signal-to-pilot power ratio is determined when the transmitted power is shared between the communication signal and the pilot tone.

BG contributed to formulating the research questions, conducted the com-

plete theoretical analysis throughout the paper, performed all the simulations, and wrote the paper.

5.2 Paper B

Björn Gävert, Mikael Coldrey, Thomas Eriksson
Phase noise estimation in OFDM systems
Published in IEEE Transactions on Communications,
Early Access

A comprehensive foundation for the theory and practice of pilot-based carrier phase synchronization of OFDM symbols in the presence of phase noise is presented. The system accounts for phase noise introduced at both the transmitter and receiver, along with the effects of a frequency-selective channel. A novel, low-complexity phase noise estimation method is proposed, which achieves near-optimal performance over a wide dynamic range of phase noise.

BG contributed to formulating the research questions, conducted the complete theoretical analysis throughout the paper, performed all the simulations, and wrote the paper.

5.3 Paper C

Björn Gävert, Mikael Coldrey, Thomas Eriksson
Analysis and Mitigation of Phase Noise in a Line-Of-Sight MIMO System
Submitted to IEEE Transactions on Communications.

A solid foundation for the theory and practice of pilot-based carrier phase synchronization in line-of-sight MIMO systems affected by phase noise is presented. To maximize the data rate, a novel pilot-based MMSE estimator is formulated, jointly estimating the received symbols and the unknown phase noise at both the transmitter and receiver. Furthermore, it is shown that power allocation, considering phase noise effects, plays a crucial role in maximizing the rate of phase-noise-limited systems.

BG contributed to formulating the research questions, conducted the com-

plete theoretical analysis throughout the paper, performed all the simulations, and wrote the paper.

CHAPTER 6

Concluding Remarks and Future Work

The pilot-based methods proposed in Papers A to C cover a wide range of systems. Close-to-optimal phase noise estimators are introduced, and several aspects related to maximizing the rate of the communication signal are explored. Further research on purely pilot-based carrier phase noise estimation is unlikely to provide significant additional performance benefits.

Further research on phase estimation based on unknown payload is of interest for reducing residual phase noise distortion without increasing pilot overhead or complexity. This includes developing innovative approaches to avoid methods that suffer from exploding complexity due to uncertainties in the user payload. A combination of clever approximations and new insights could lead to low-complexity, high-performance, user-payload-based phase estimators that complement purely pilot-based phase estimators.

As mentioned in Chapter 1, carrier phase noise is a significant source of distortion in both current and future radio systems. Furthermore, there is growing interest in wideband communication, with wireless communication equipment operating at higher carrier frequencies. As the demand for higher data rates increases, radio systems either become more complex (e.g., MIMO) or use wireless communication signals with larger bandwidths, often at higher

carrier frequencies, all of which result in systems suffering from phase noise.

Systems with increased complexity include, for example, distributed massive MIMO systems. Phase synchronization becomes a challenge when coordinating wireless transmission and reception in a distributed radio network, and it becomes a significant issue if the data traffic to and from the distributed radio units relies on wireless transmission. Further research in this area is needed.

It is of interest to study wideband MIMO at higher carrier frequencies, where, for example, LOS-MIMO in the D-band (110–170 GHz) could offer a potential solution for achieving terabits per second (Tbps) rates. Given the high bandwidth, digital signal processing solutions with low complexity and high performance are crucial.

Wireless communication signals with significant bandwidth primarily suffer from white phase noise. The low-frequency colored component of the phase noise is negligible compared to the white noise floor of the oscillators over the wide bandwidth of the communication signal. With white phase noise, phase noise estimation becomes ineffective, and alternative methods, such as optimal signal shaping, must be explored to mitigate phase noise distortion.

Integration is a key factor in reducing equipment power consumption and costs, and enabling technologies like massive MIMO with fully digital precoding and combining. As integration increases, digital interfaces are moving closer to the antennas, where digital-to-analog converters (DACs) and analog-to-digital converters (ADCs) are used for direct RF generation and sampling. As DACs and ADCs become more tightly integrated with the antenna, traditional phase noise from up- and down-conversion translates into timing jitter within the converters. With the growing demand for higher carrier frequencies and increased bandwidths, further research into modeling and managing timing jitter in DACs and ADCs, particularly its impact on both carrier phase noise and symbol jitter, is becoming increasingly important.

References

[1] M. Shafi, A. F. Molisch, P. J. Smith, *et al.*, "5G: A tutorial overview of standards, trials, challenges, deployment, and practice," *IEEE Journal on Selected Areas in Communications*, vol. 35, pp. 1201–1221, 6 Jun. 2017, ISSN: 07338716.

[2] W. Chen, X. Lin, J. Lee, *et al.*, "5G-Advanced Toward 6G: Past, Present, and Future," *IEEE Journal on Selected Areas in Communications*, vol. 41, pp. 1592–1619, 6 Jun. 2023, ISSN: 15580008.

[3] H. Tataria, M. Shafi, A. F. Molisch, M. Dohler, H. Sjoland, and F. Tufvesson, "6G Wireless Systems: Vision, Requirements, Challenges, Insights, and Opportunities," *Proceedings of the IEEE*, vol. 109, pp. 1166–1199, 7 Jul. 2021, ISSN: 15582256.

[4] Ericsson, "Ericsson Mobility Report," Tech. Rep., 2024.

[5] Q. Wu, G. Y. Li, W. Chen, D. W. K. Ng, and R. Schober, *An Overview of Sustainable Green 5G Networks*, 2017.

[6] U. Gustavsson, P. Frenger, C. Fager, *et al.*, "Implementation Challenges and Opportunities in Beyond-5G and 6G Communication," *IEEE Journal of Microwaves*, vol. 1, pp. 86–100, 1 2021.

[7] T. H. Lee and A. Hajimiri, "Oscillator phase noise: A tutorial," *IEEE Journal of Solid-State Circuits*, vol. 35, pp. 326–335, 3 2000, ISSN: 00189200.

[8] Z. Chang, Y. Xu, J. Chen, N. Xie, Y. He, and H. Li, "Modeling, Estimation, and Applications of Phase Noise in Wireless Communications: A Survey," *IEEE Communications Surveys and Tutorials*, 2024, ISSN: 1553877X.

[9] A. F. Molisch, *Wireless communications https://researchpapers4scolars.files.wordpress.com/2015/06 /andreas-f-molisch-wireless-comm.pdf*. Wiley : IEEE, 2011, p. 827, ISBN: 9780470741870.

[10] L. Tong, B. M. Sadler, and M. Dong, "Pilot-assisted wireless transmissions: general model, design criteria, and signal processing," *IEEE Signal Processing Magazine*, 6 Nov. 2004.

[11] A. Lapidoth, *A Foundation In Digital Communication*, Second. Cambridge University Press, 2017.

[12] G. Colavolpe, A. Barbieri, and G. Caire, "Algorithms for iterative decoding in the presence of strong phase noise," *IEEE Journal on Selected Areas in Communications*, vol. 23, pp. 1748–1757, 9 Sep. 2005, ISSN: 07338716.

[13] A. Spalvieri and L. Barletta, "Pilot-aided carrier recovery in the presence of phase noise," *IEEE Transactions on Communications*, vol. 59, pp. 1966–1974, 7 Jul. 2011, ISSN: 00906778.

[14] P. Mathecken, T. Riihonen, S. Werner, and R. Wichman, "Phase Noise Estimation in OFDM: Utilizing Its Associated Spectral Geometry," *IEEE Transactions on Signal Processing*, vol. 64, pp. 1999–2012, 8 Apr. 2016, ISSN: 1053587X.

[15] R. A. Casas, S. L. Biracree, and A. E. Youtz, "Time domain phase noise correction for OFDM signals," *IEEE Transactions on Broadcasting*, vol. 48, pp. 230–236, 3 2002, ISSN: 00189316.

[16] E. G. Larsson, O. Edfors, F. Tuvfesson, and T. L. Marzetta, "Massive MIMO for Next Generation Wireless Systems," *IEEE Communications Magazine*, vol. 52, p. 186, 2 Feb. 2014.

[17] P. Larsson, "Lattice array receiver and sender for spatially orthonormal MIMO communication," *IEEE 61st Vehicular Technology Conference*, 2005.

[18] X. Song and G. Fettweis, "On Spatial Multiplexing of Strong Line-of-Sight MIMO with 3D Antenna Arrangements," *IEEE Wireless Communications Letters*, vol. 4, pp. 393–396, 4 2015, ISSN: 21622345.

[19] L. Barletta, F. Bergamelli, M. Magarini, N. Carapellese, and A. Spalvieri, "Pilot-aided trellis-based demodulation," *IEEE Photonics Technology Letters*, vol. 25, pp. 1234–1237, 13 2013, ISSN: 10411135.

[20] A. Tarable, G. Montorsi, S. Benedetto, and S. Chinnici, "An EM-based phase-noise estimator for MIMO systems," in *International Conference on Communications (ICC)*, IEEE, Jun. 2013, ISBN: 9781467331227.

[21] A. A. Nasir, H. Mehrpouyan, R. Schober, and Y. Hua, "Phase noise in MIMO systems: Bayesian Cramér-Rao bounds and soft-input estimation," *IEEE Transactions on Signal Processing*, vol. 61, pp. 2675–2692, 10 2013, ISSN: 1053587X.

[22] W. Rave, D. Petrovic, and G. Fettweis, "Iterative Correction of Phase Noise in Multicarrier Modulation," *Proc. 9th Int. OFDM Workshop*, 2004.

[23] D. Petrovic, W. Rave, and G. Fettweis, "Effects of phase noise on OFDM systems with and without PLL: characterization and compensation," *IEEE Transactions On Communications*, vol. 55, 8 2007.

[24] S. Wu, P. Liu, and Y. Bar-Ness, "Phase noise estimation and mitigation for OFDM systems," *IEEE Transactions on Wireless Communications*, vol. 5, pp. 3616–3625, 12 Dec. 2006, ISSN: 15361276.

[25] M. R. Khanzadi, R. Krishnan, and T. Eriksson, "Estimation of phase noise in oscillators with colored noise sources," *IEEE Communications Letters*, vol. 17, pp. 2160–2163, 11 Nov. 2013, ISSN: 10897798.

[26] A. Demir, A. Mehrotra, and J. Roychowdhury, "Phase noise in oscillators: a unifying theory and numerical methods for characterization," *IEEE Transactions on Circuits and Systems I: Fundamental Theory and Applications*, vol. 47, pp. 655–674, 5 2000, ISSN: 10577122.

[27] J. Eatwell, M. Millgate, and P. Newman, *Time Series and Statistics https://link.springer.com/book /10.1007/978-1-349-20865-4*. Palgrave Macmillan UK, 1990.

[28] S. Mandelli, M. Magarini, and A. Spalvieri, "Modeling the filtered and sampled continuous-time signal affected by wiener phase noise," *2014 19th European Conference on Networks and Optical Communications, NOC 2014*, pp. 173–178, Dec. 2014.

[29] A. Puglielli, G. Lacaille, A. M. Niknejad, G. Wright, B. Nikolic, and E. Alon, "Phase noise scaling and tracking in OFDM multi-user beamforming arrays," *IEEE International Conference on Communications, ICC 2016*, 2016.

[30] A. Spalvieri and M. Magarini, "Wiener's analysis of the discrete-time phase-locked loop with loop delay," *IEEE Transactions on Circuits and Systems II: Express Briefs*, vol. 55, pp. 596–600, 6 2008, ISSN: 15583791.

[31] S. M. Kay, *Statistical Signal Processing: Estimation Theory*, 20th. Prentice Hall PTR, 2013, p. 596, ISBN: 0-13-345711-7.

[32] A. Piemontese, G. Colavolpe, and T. Eriksson, "A New Analytical Model of Phase Noise in Communication Systems," in *IEEE Wireless Communications and Networking Conference, WCNC*, vol. 2022-April, Institute of Electrical and Electronics Engineers Inc., 2022, pp. 926–931, ISBN: 9781665442664.

[33] F. Zhang, Y. Li, J. Wu, W. Li, X. Hong, and J. Lin, "Improved pilot-aided optical carrier phase recovery for coherent M-QAM," *IEEE Photonics Technology Letters*, vol. 24, pp. 1577–1580, 18 2012, ISSN: 10411135.

[34] J. Lin, Z. Zhang, L. Xi, and X. Zhang, "Pilot-tone-aided two-stage carrier phase recovery in dual-carrier nyquist m-QAM transmission system," in *Conference on Lasers and Electro-Optics Europe - Technical Digest*, vol. 2014-Janua, 2014.

[35] Z. Liu, J. Y. Kim, D. S. Wu, D. J. Richardson, and R. Slavik, "Homodyne OFDM with optical injection locking for carrier recovery," *Journal of Lightwave Technology*, vol. 33, pp. 34–41, 1 Jan. 2015, ISSN: 07338724.

[36] Z. Zhang, J. Lin, X. Su, L. Xi, Y. Qiao, and X. Zhang, "Optical domain scheme of pilot-tone-aided carrier phase recovery for Nyquist single-carrier optical communication system," *Optical Engineering*, vol. 53, p. 066 108, 6 Jun. 2014, ISSN: 0091-3286.

[37] G. Liu and W. Zhu, "Compensation of phase noise in OFDM systems using an ICI reduction scheme," *IEEE Transactions on Broadcasting*, vol. 50, pp. 399–407, 4 Dec. 2004, ISSN: 00189316.

[38] V. Syrjala, T. Levanen, T. Ihalainen, and M. Valkama, "Pilot Allocation and Computationally Efficient Non-Iterative Estimation of Phase Noise in OFDM," *IEEE Wireless Communications Letters*, vol. 8, pp. 640–643, 2 Apr. 2019, ISSN: 21622345.

[39] P. Mathecken, T. Riihonen, S. Werner, and R. Wichman, "Constrained phase noise estimation in OFDM using scattered pilots without decision feedback," *IEEE Transactions on Signal Processing*, vol. 65, pp. 2348–2362, 9 May 2017, ISSN: 1053587X.

[40] H. Abdi and L. J. Williams, *Principal component analysis*, Jul. 2010.

[41] E. B. Slimane, S. Jarboui, and A. Bouallègue, "Blind phase synchronization for multiple-antenna systems," in *International Wireless Communications and Mobile Computing Conference (IWCMC)*, IEEE, Sep. 2016, ISBN: 9781509003044.

[42] N. Hadaschik, M. Dörpinghaus, A. Senst, *et al.*, "Improving MIMO phase noise estimation by exploiting spatial correlations," in *IEEE International Conference on Acoustics, Speech, and Signal Processing*, May 2005.

[43] L. Reggiani, G. Filiberti, and L. Dossi, "Phase Noise Suppression in MIMO LoS Systems for High Capacity Backhauling," *Wireless Personal Communications*, vol. 82, pp. 1931–1953, 3 Jun. 2015, ISSN: 1572834X.

[44] G. Bishop and G. Welch, "An Introduction to the Kalman Filter," Department of Computer Science, University of North Carolina, Tech. Rep., 2001.

[45] M. A. Khalighi, J.-M. Brossier, G. Jourdain, and K. Raoof, "Water Filling Capacity of Rayleigh MIMO Channels," in *12th IEEE International Symposium on Personal, Indoor and Mobile Radio Communications. PIMRC 2001. Proceedings*, 2001.

[46] B. Gavert and T. Eriksson, "Estimation of Phase Noise Based on In-Band and Out-of-Band Frequency Domain Pilots," *IEEE Transactions on Communications*, vol. 70, pp. 4780–4792, 7 Jul. 2022, ISSN: 15580857.

[47] B. Gavert, M. Coldrey, and T. Eriksson, “Phase noise estimation in OFDM systems,” *IEEE Transactions on Communications*, 2024, ISSN: 15580857.